Non-integrable systems with algebraic singularities in complex time

1991 J. Phys. A: Math. Gen. 24 3217

(http://iopscience.iop.org/0305-4470/24/14/011)

J. Phys. A: Math. Gen. **24** (1991) 3217–3236. Printed in the UK

Non-integrable systems with algebraic singularities in complex time

T Bountis†, L Drossos† and I C Percival‡

† Department of Mathematics, University of Patras, Patras 26110, Greece
‡ School of Mathematical Sciences, Queen Mary and Westfield College, University of London, Mile End Road, London E1 4NS, UK

Received 10 January 1991

Abstract. Dynamical arguments are presented which suggest that there are non-integrable systems without clustering of singularities, without infinite singularities, or singularities with an infinite number of branches in the complex t-plane. Several examples with only algebraic singularities are studied, for which strong numerical evidence is presented for non-integrability and infinitely sheeted solutions. 'Weak-Painlevé' potentials are also analysed from this point of view, and all integrable cases are found to possess only finitely sheeted solutions.

1. Introduction

It has been widely suggested, on the basis of apparently overwhelming evidence, that infinite branching and clustering of singularities of the configuration coordinates in the complex t-plane is a 'universal' feature of non-integrable dynamical systems [1–7]. Although some isolated examples of non-integrable systems with finite branching [6] and absence of clustering [7, 8] have been reported in the literature, a more comprehensive analysis and deeper understanding of such systems has been lacking.

In this paper, we first present physical arguments suggesting that there is a large class of non-integrable Hamiltonian systems with only algebraic singularities in complex time. We then proceed to study the analytic structure of several of these examples in the t-plane and present evidence of their infinitely sheeted solutions (ISS). Furthermore, we show how finite-sheetedness and ISS can be used to distinguish between integrable and non-integrable systems whose solutions contain only rational powers of t, when expanded about a singularity at $t = t_*$.

The Hamiltonian systems studied in this paper have the standard form

$$H(x, y, p_x, p_y) = \tfrac{1}{2}(p_x^2 + p_y^2) + V(x, y) \tag{1.1}$$

which describes a particle of unit mass moving in a two-dimensional potential V. In particular, we shall investigate here the following examples:

$$\text{(i)} \qquad V(x, y) = \frac{k}{(f(x, y))^2} + \tfrac{1}{2}(Ax^2 + By^2) \qquad k, A, B > 0 \tag{1.2}$$

0305-4470/91/143217+20$03.50

with

$$f(x,y)=\begin{cases}(x-y) & (1.3a)\\ (x^2+y^2-1)^2 & (1.3b)\\ (x^2+y^2+1)^2 & (1.3c)\end{cases}$$

where (1.2) with (1.3*a*) belongs to a class of Calogero-Moser potentials [9], (1.3*b*) corresponds to a problem of 'soft billiards' [10] and (1.3*c*) gives a smooth potential (1.2) for all real (x, y).

(ii) $$V(x,y)=\tfrac{1}{8}x^4+\tfrac{3}{4}x^2y^2+y^4+\lambda x \qquad (1.4)$$

first studied by Grammaticos *et al* [11], which is integrable for $\lambda=0$ and has only algebraic singularities for $\lambda\neq 0$.

We demonstrate analytically that the above potentials have only square root singularities in the solutions $(x(t), y(t))$, for complex t, and present strong numerical evidence for their non-integrability and the existence of ISS in every case. The analytic structure of these potentials is subsequently compared with that of the weak-Painlevé examples [6]

(iii) $$V(x,y)=\begin{cases}y^5+y^3x^2+\frac{3}{16}yx^4 & (1.5a)\\ y^6+\frac{5}{4}x^2y^4+\frac{3}{8}x^4y^2+\frac{1}{64}x^6 & (1.5b)\end{cases}$$

which are known to be completely integrable and possess only rational powers of t in the expansions of their solutions around a singularity.

In section 2 we address the issues of infinite branching and clustering of singularities and present dynamical arguments, which cast doubt on earlier interpretations of the significance of these issues. Furthermore, we suggest that there is a large class of non-integrable systems with no more than algebraic singularities in the complex t-plane.

Section 3 examines one example which is a perturbation of an important class of integrable systems with only square root singularities: a two-particle Calogero-Moser potential with quadratic terms. We give the explicit solution in the integrable $(A=B)$ case and integrate the equations of motion numerically in the complex t-plane, for $A\neq B$, to show that they have ISS around contours enclosing two pairs of complex conjugate singularities. Then in section 4 we study the solutions of (1.2) with (1.3*b*) and other related potentials with only square root singularities and find similar evidence of ISS for $A\neq B$, in every case.

In section 5, we turn to potential (1.4), whose square root singularities are infinite (i.e. occur at finite $t=t_*$ at which (x, y) becomes infinite). Here also, in the non-integrable case $\lambda\neq 0$, the branches of these singularities appear to be connected in such a way that ISS is observed in the same way, integrating around suitably large contours in the complex t-plane.

It is interesting to compare these results with the ones obtained in section 6, where we have analysed, from the same point of view, two completely integrable systems with algebraic singularities: the weak-Painlevé potentials (1.5*a*, *b*) for which we find finitely sheeted solutions in every case.

Finally, our conclusions are presented in section 7, with a more detailed discussion of our numerical and analytical results given in appendices 1 and 2 respectively.

2. Dynamical interpretation of singularities

Many properties of dynamical systems in the complex t-plane can be discussed in dynamical terms, just as if t were real, though some minor modifications are needed.

Suppose $\boldsymbol{r}(t) = (x(t), y(t))$ is a complex analytic solution of the equations of motion for the configuration variables x, y of the Hamiltonian system (1.1). If the particle reaches an infinite value of $\boldsymbol{r}$ in finite real time, then $V(\boldsymbol{r})$ must diverge faster than a quadratic for large $\boldsymbol{r}$. The same is true for complex time. The difference between real and complex t is that for real t, $V(\boldsymbol{r})$ must be negative, whereas for complex t there is no constraint on the sign of $V(\boldsymbol{r})$.

We shall call a singularity of $\boldsymbol{r}(t)$, at $t = t_*$, an *infinite* singularity, if $\boldsymbol{r}(t)$ is unbounded in the neighbourhood of $t = t_*$. Otherwise it will be called a finite singularity. Now we may use the form of $V(\boldsymbol{r})$ to study the dynamical properties of the motion in the following way.

If the singularity at $t = t_*$ is infinite and t_* is finite, this means that the particle reaches an infinite value of $\boldsymbol{r}$ in finite complex time. Thus, the occurrence of infinite singularities is connected with the properties of V and the dynamics of the system in the limit of large $\boldsymbol{r}$.

Now suppose that there are two infinite singularities in $\boldsymbol{r}(t)$, one at $t = t_a$ and one at $t = t_b$, on the same sheet of the complex plane. This means, dynamically, that the particle can go from infinity to infinity in a finite complex time interval of magnitude $|t_a - t_b|$. Furthermore, if infinite singularities cluster, the particle can go from infinity to infinity in arbitrarily short times.

Why should the integrability of a system depend on some special property of the dynamics at infinity? A little thought shows that this commonly encountered consideration of singularities at infinity is due to the usual choice of potentials $V(\boldsymbol{r})$, which are analytic for all finite values of $\boldsymbol{r}$. For such potentials, all singularities in the complex t-plane must be infinite. Hence, the motion of a non-integrable system which is free from such singularities cannot be governed by a potential $V(\boldsymbol{r})$, which is an entire complex function of $\boldsymbol{r}$. It must therefore have a $V(\boldsymbol{r})$ which possesses singularities at *finite* $\boldsymbol{r}$.

Now consider a singularity at $t = t_*$, for which the value $\boldsymbol{r}_* = \boldsymbol{r}(t_*)$ is finite. Since $\boldsymbol{r}(t)$ is analytic in the neighbourhood of values of $\boldsymbol{r}$ for which $V(\boldsymbol{r})$ is analytic, it follows that $V(\boldsymbol{r})$ must be singular at $\boldsymbol{r} = \boldsymbol{r}_*$. Thus, *this type of singularity in* $\boldsymbol{r}(t)$ depends on the type of singularity in $V(\boldsymbol{r})$.

For non-integrable systems, Ziglin's theorem [6, 12] tells us that there must exist solutions with an infinite number of sheets. These sheets are, of course, joined at the singularities. It is an open question, however, as to how this property of ISS manifests itself in systems whose singularities are all finitely branched.

We will start by examining non-integrable Hamiltonian systems (1.1) with the following properties:

(i) $V(\boldsymbol{r})$ must diverge at infinity no faster than a quadratic in x and y;

(ii) the potential $V(\boldsymbol{r})$ must be singular for, at least, one finite value of $\boldsymbol{r}$, not necessarily real;

(iii) at least one of the singularities in the potential must produce a branch cut in $\boldsymbol{r}(t)$.

The simplest singularity with a branch cut is the square root singularity. For motion in one dimension a square root singularity in $x(t)$ at $x = x_*$ is produced by the inverse square potential $\sim k/(x - x_*)^2$. Thus, for simplicity, we shall first seek non-integrable dynamical systems with the additional property:

(iv) the potential $V(r)$ has only singularities at (x, y) where the term with the inverse square of $f(x, y)$ in (1.2) diverges.

3. Singularity analysis of a Calogero–Moser system

There is a large class of Hamiltonian systems of many degrees of freedom with all the properties (i)-(iv) listed above, which are known as Calogero-Moser systems [9]. In the case of two degrees of freedom the potential $V(x, y)$ of an example of such a Hamiltonian system has the form

$$V(x, y) = \frac{k}{(x-y)^2} + \tfrac{1}{2}(Ax^2 + By^2) \qquad k, A, B > 0 \tag{3.1}$$

and is completely integrable only in the symmetric case $A = B$. The equations of motion are

$$\ddot{x} = -Ax + \frac{2k}{(x-y)^3} \qquad \ddot{y} = -By - \frac{2k}{(x-y)^3}. \tag{3.2}$$

Note that, for $A = B$, (3.2) uncouple under the transformation

$$z = x - y \qquad w = x + y \tag{3.3}$$

into

$$\ddot{w} = -Aw \qquad \ddot{z} = -Az + \frac{4k}{z^3} \tag{3.4}$$

and hence possess the additional integral

$$\tfrac{1}{2}\dot{z}^2 + \tfrac{1}{2}Az^2 + \frac{2k}{z^2} = F = \text{const} \tag{3.5}$$

which is in involution with the Hamiltonian.

It is not difficult to integrate the second equation in (3.4) explicitly, starting with the integral (3.5), and derive

$$z^2 = \frac{1}{\sqrt{A}}\left[F + \left(\frac{F^2}{A} - 4k\right)^{1/2} \sin[2\sqrt{A}\,(t - t_0)]\right] \tag{3.6}$$

where t_0 is a second arbitrary constant. This confirms analytically that, in the case $A = B$, our solutions (3.3) possess exactly two Riemann sheets corresponding to the $\pm$ choice in taking the square root of (3.6).

The *local* two-sheetedness of solutions can also be revealed, by direct singularity analysis, even when analytical solutions like (3.6) are not available. Thus, for general A and B, one can expand $x(t)$ and $y(t)$ near a (movable) singularity $t = t_*$ of (3.2) and show that the *only leading behaviour* allowed is of the form

$$x = \alpha + c_1\tau^{1/2} + \ldots \qquad y = \alpha + c_2\tau^{1/2} + \ldots \qquad \tau = t - t_* \tag{3.7}$$

where α is a free constant and $c_1 = -c_2 = (-k)^{1/4}$. The only type of singularity, therefore, in this problem occurs when the equations of motion themselves are singular, at $x - y = 0$. These singularities are, of course, *finite*, since the configuration variables $x(t)$, $y(t)$ are finite at $t = t_*$ (it is the velocities $\dot{x}(t)$, $\dot{y}(t)$ and their derivatives that blow up as $t \to t_*$).

However, it is not yet clear from (3.7) alone that the above singularities are of the square root type. One needs to expand (3.7) to higher order to see whether singularities of the logarithmic type arise, where further arbitrary constants enter in (3.7) [6]. To find out whether this occurs, let us insert in (3.2) x, y in the form

$$x = \alpha + c_1\tau^{1/2} + d_1\tau^{r+1/2} \qquad y = \alpha + c_2\tau^{1/2} + d_2\tau^{r+1/2} \qquad \tau = t - t_* \tag{3.8}$$

and seek to determine the orders, r, at which the coefficients d_1 and/or d_2 are *arbitrary*. This takes place at r values, at which the determinant of $\boldsymbol{M}$ in the linear system

$$\boldsymbol{M}\boldsymbol{d} = \boldsymbol{g} \qquad \boldsymbol{d} = \begin{bmatrix} d_1 \\ d_2 \end{bmatrix} \qquad \boldsymbol{g} = \begin{bmatrix} g_1 \\ g_2 \end{bmatrix} \tag{3.9}$$

vanishes, i.e. where

$$\det \boldsymbol{M} = (r+1)(r-1)(r^2 - \tfrac{1}{4}) = 0. \tag{3.10}$$

The root $r = -1$ is due to the arbitrary location of the singularity $t = t_*$ and $r = -\frac{1}{2}$ corresponds to the free constant α in (3.7), (3.8). It remains to check whether at $r = \frac{1}{2}$, 1, i.e. at terms of order τ and $\tau^{3/2}$ in (3.8), the RHS $\boldsymbol{g}$ of (3.9) is such that $\log\tau$ terms are required to satisfy the corresponding compatibility conditions.

Note, however, that upon second differentiation, the τ, $\tau^{3/2}$ terms in (3.8) will enter on the LHS of (3.2) at orders *lower* than constant, which is the leading order of the linear terms $-Ax$, and $-By$ on the RHS of (3.2). Thus, these linear terms (and hence the parameters A and B, be they equal or not) will *not* alter the nature of the singularity, which is determined completely by the terms of lower order. These terms (at orders τ^{-1} and $\tau^{-1/2}$), yield $g_1 = g_2 = 0$ in (3.9), and hence do not introduce any logarithms, as the series solutions (3.8) of the problem finally become

$$\begin{aligned} x &= \alpha + (-k)\tau^{1/4} + d\tau + f\tau^{3/2} + \sum_{n=4}^{\infty} a_n\tau^{n/2} \\ y &= \alpha - (-k)\tau^{1/4} + d\tau - f\tau^{3/2} + \sum_{n=4}^{\infty} b_n\tau^{n/2} \end{aligned} \tag{3.11}$$

with t_*, a, d and f providing the complete set of the free constants to be specified by the initial conditions of the problem.

Now that the nature of the singularities of the Calogero–Moser system (3.1) has been determined, we proceed to investigate their location and arrangement in the complex t-plane. In the integrable case $A = B$ this is easy. Since these singularities correspond to $z = x - y = 0$, we can obtain them directly from (3.6):

$$t_* = t_0 - \frac{1}{2\sqrt{A}}\left[\sin^{-1}\left(\frac{F}{\sqrt{F^2/A - 4k}}\right) + m\pi\right] \tag{3.12}$$

where m is any integer and t_0, F are determined by the initial conditions. This shows that the singularities of this system are located periodically along two rows parallel to the $\mathrm{Re}(t)$ axis intersecting the $\mathrm{Im}(t)$ axis at $t_I = \pm\mathrm{Im}(t_*)$, as shown in figure 1 (for every singularity of x, y at $t = t_*$, there is one of x, y at $t = \bar{t}_*$).

Locally, of course, around any contour C_1 enclosing one singularity, the solutions of the system return to their starting values after two turns. Integrating now along larger contours C_2, C_3, etc. (see figure 1), in the *integrable* case $A = B$, all solutions repeat after only one or two turns, depending on whether the number of singularities enclosed is even or odd. This is because in that case the general solution is available in closed form, cf (3.6), and has globally also a very simple sheet structure.

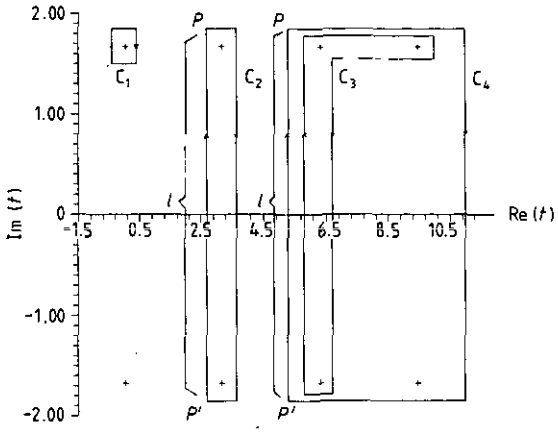

Figure 1. Locations of singularities on the primary Riemann sheet and several paths of integration around them, in the integrable case of Calogero–Moser system (3.1) with $A = 1$, $B = 1$, $E = 3.5$.

The interesting question is: what happens when $A \neq B$? Integrating the equations of motion (3.2) numerically in that case, and plotting the intersections of the orbits with the Poincare surface of section x, $\dot{x}$ ($y = 0$, $\dot{y} \geqslant 0$), large-scale chaotic behaviour is observed, strongly indicating that the problem is *non-integrable* (see figure 2). How is this global property of the system reflected by the analytic structure of the solutions in the complex t-plane?

A theorem of S L Ziglin's [6, 12] assures us that non-integrable Hamiltonian systems must have ISS. Our objective, therefore, is to find out in what way do ISS occur in this problem, when $A \neq B$. Locally, of course, around a contour C_1 enclosing only one singularity, all solutions retain their two-sheeted structure, as indicated by their expansions (3.11), which are valid for sufficiently small τ.

The answer must lie, therefore, in the more *global* solutions, around contours enclosing *more than one* singularity in the complex t-plane. Indeed, when we integrated

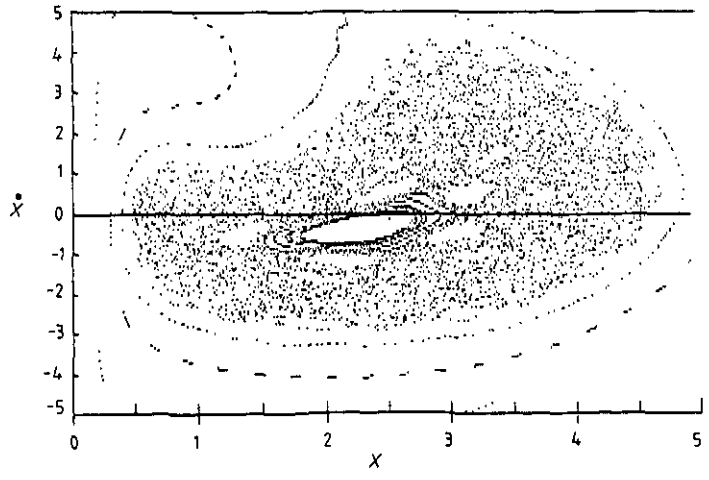

Figure 2. Surface of section for Hamiltonian (1.1) with potential (3.1) in the case $A = 1$ $B = 4$, $E = 20$.

(3.2) around contours C_2, C_3, etc. (see figure 1), *new* singularities started appearing on other sheets, causing the solutions to repeat after more and more turns N, as the 'height' l of our rectangular contours kept increasing, as shown in figure 3. All our

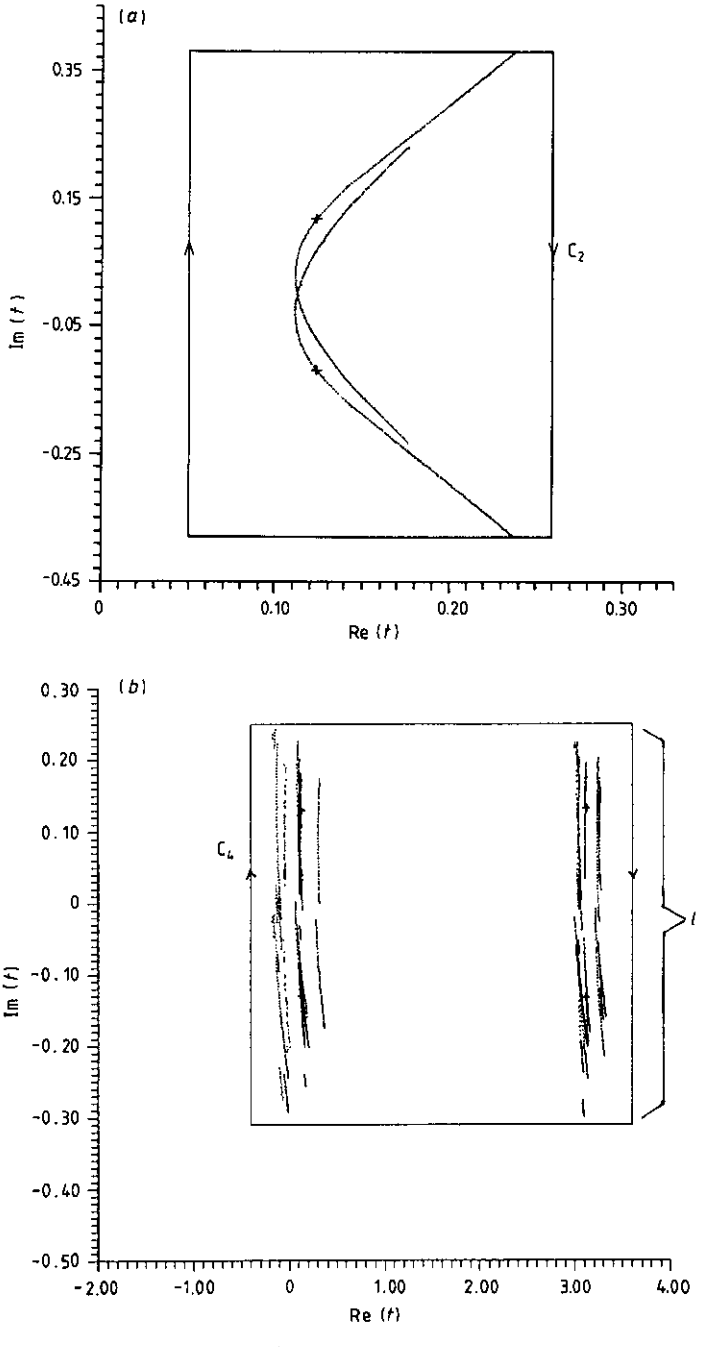

Figure 3. Singularity patterns in the complex t-plane of the Calogero–Moser system when one integrates around (*a*) contour C_2 of figure 1 (300 times) for $A=1$, $B=1.15$, $E=10$, and (*b*) contour C_4 at $A=1$, $B=1.15$, $E=10$.

integrations in the complex t-plane were carried out using the ATOMFT package developed by Chang and Corliss [13].

In this problem, taking $A=1$ and varying B, we found that integrating around contours enclosing two singularities, the solutions always returned to their starting values, after a number of turns N that grows on the average linearly with l (see figure 4(a)). However, when we turned around contours enclosing four singularities (see figure 3(b)) the solutions did not exactly repeat but exhibited *near returns* to their starting values after a number of turns N that also appeared to increase linearly with l (see figure 4(b)).

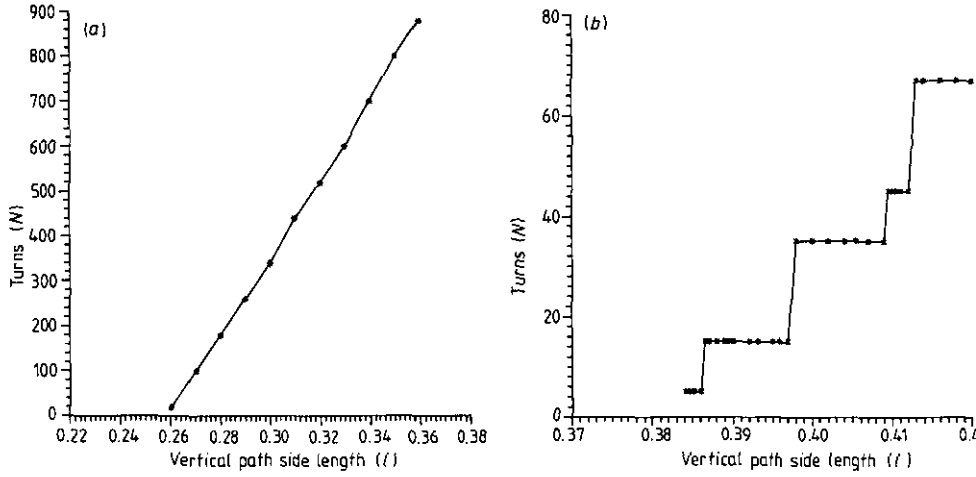

Figure 4. (a) Plot of the number of turns N needed to (exactly) return to the original Riemann sheet versus the length of the vertical side of contour C_2, containing one pair of singularities, for the non-integrable Calogero–Moser system at $A=1$, $B=1.01$, $E=21$. (b) Same as (a) for contour C_4, containing two pairs of singularities, with $A=1$, $B=2$, $E=3.5$.

The absolute differences, after N turns, in the values of solutions from their initial conditions were observed to grow steadily as B was changed further away from unity (see also discussion in appendix 1). All this suggests that, in the non-integrable case, ISS are indeed observed around such contours, in a very similar way as has already been found for other potentials having only square root singularities (see [10] and section 4 below).

Thus, non-integrable dynamical systems with only algebraic singularities in t and ISS certainly do exist. Moreover, these singularities exhibit *no clustering* and are distributed on different sheets, as seen in figure 3 where only their projection on one sheet is shown.

4. The soft billiard and other related potentials

Let us now investigate, from the same point of view, the analytic structure of the solutions of (1.1) with $V(x, y)$ given by (1.2), with (1.3b), i.e.

$$V(x, y)=\frac{k}{(x^2+y^2-1)^2}+\tfrac{1}{2}(Ax^2+By^2) \qquad k, A, B>0 \tag{4.1}$$

which is integrable for $A = B$ by virtue of rotational symmetry. Just as in the Calogero-Moser system of section 3, this problem also has only square root singularities (created by the inverse square part of the potential) near which its solutions are of the form

$$x = x_* + a_1\tau^{1/2} + \ldots \qquad y = y_* + a_2\tau^{1/2} + \ldots \qquad \tau = t - t_* \tag{4.2}$$

where $\tau = t - t_*$ and $x_*^2 + y_*^2 = 1$. One can easily carry out the singularity analysis and check that, for $A = B$, the series expansions of the solutions (1.2), near such a singularity, contain four arbitrary constants and only powers of $\tau^{1/2}$ to all orders.

The analytical solution of the equations of motion

$$\ddot{x} = -Ax + \frac{2k}{(x^2+y^2-1)^3} \qquad \ddot{y} = -By - \frac{2k}{(x^2+y^2-1)^3} \tag{4.3}$$

in the $A = B$ case can be derived in an implicit form after transforming to polar coordinates $x = r\cos\theta$, $y = r\sin\theta$ and introducing the new variable $u = r^2 - 1$:

$$t - t_0 = \pm\tfrac{1}{2}\int_{u_0}^{u} \frac{u\,du}{\sqrt{2E(u+1)u^2 - A(u+1)^2u^2 - J^2u^2 - 2k(u+1)}} \tag{4.4}$$

where $J = r^2\dot{\theta} = \text{const}$ is the angular momentum integral and E is the total energy. The integration in (4.4) can be carried out in terms of elliptic integrals of the first and third kinds (see appendix 2), which are in general quite difficult to invert in order to obtain r, θ (and hence x, y) as functions of t [14]. However, as we discuss in appendix 2, closed-form solutions also exist in some special cases which can further illuminate the analytic structure of the integrable problem.

There are, of course, many different kinds of perturbations of the $A = B$ potential (4.1), which can remove the rotational symmetry and make the system non-integrable. In doing so, however, care must be taken to preserve properties (i)-(iv) of section 3 as well as the finite nature of the singularities.

Thus, we chose first to perturb the denominator of (1.2) and (1.3*b*) and consider instead the potential

$$V(x, y) = \frac{k}{(x^2 + b^2y^2 - 1)^2} + \tfrac{1}{2}(Ax^2 + By^2) \tag{4.5}$$

but this led to the appearance of *logarithmic* terms in the expansion around finite singularities at points $r_* = (x_*, y_*)$ satisfying $x_*^2 + b^2y_*^2 - 1 = 0$, as follows [10]:

$$\begin{aligned} x &= x_* + a_1\tau^{1/2} + b_1\tau + [c_1 + d_1\log(\tau)]\tau^{3/2} + \ldots \\ y &= y_* + a_2\tau^{1/2} + b_2\tau + [c_2 + d_2\log(\tau)]\tau^{3/2} + \ldots \end{aligned} \tag{4.6}$$

and $\tau = t - t_*$, where now only t_* and c_1 are free constants.

The logarithmic terms in (4.6) introduce infinite branching at the singularity $t = t_*$, which we wish to avoid. So we were led to leave the denominator unchanged, and consider the potential (1.2) with (1.3*b*) and different A, B in general. These cannot have any logarithms in $r(t)$, since the contributions of Ax^2, By^2 in the series expansions enter after the last free parameter has already been determined.

Integrating the equations of motion (4.3) twice around one such singularity $t = t_*$ returns $r(t)$ to its original value, confirming that it is a singularity (locally) of the square root type. But this local analytic structure is the same for all values of the parameters A, B! So it is natural to ask how does the non-integrable case, with $A \neq B$, differ from the rotationally symmetric $A = B$ case.

To find out, we integrated (4.3) about one and two complex conjugate pairs of singularities around contours of the C_2 and C_4 type, respectively, shown in figure 1. In the integrable case, $A = B$, the solutions always returned to their starting values after a number of turns $N(l)$, which increased *linearly* with the length l of the vertical side of the contours, as seen in figure 5. The accuracy with which the initial values of the solution are repeated varies within 10^{-10}–10^{-14} (see appendix 1 for more details).

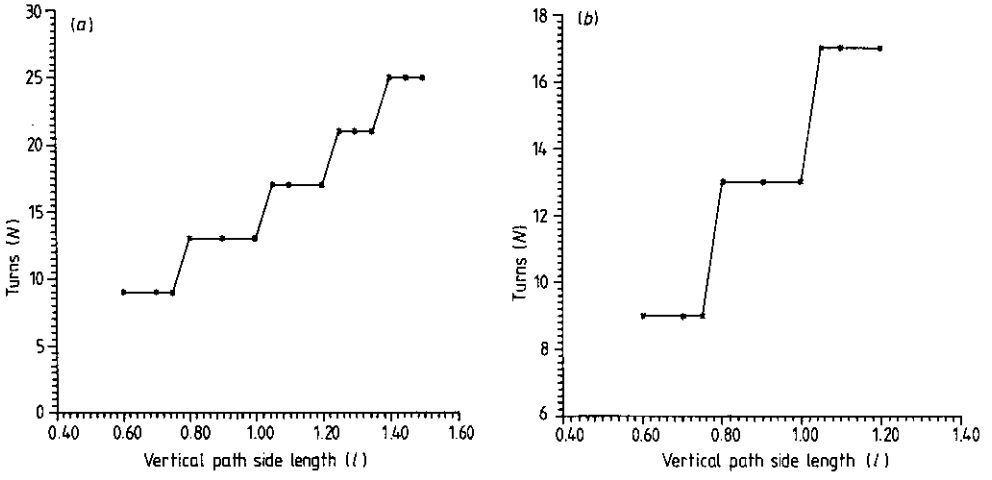

Figure 5. (*a*) Same as figure 4(*a*) for the non-integrable soft billiard potential (4.1), with $A = 1$, $B = 1.1$, $E = 10$. (*b*) Same as figure 4(*b*) for the non-integrable soft billiards system with $A = 1$, $B = 1.01$, $E = 10$.

An interesting thing happened, however, when we performed the same integrations for $A \neq B$: as in the non-integrable case of the Calogero–Moser system of section 3, around two complex conjugate pairs of singularities, the solutions came close to their starting values, with an accuracy that became smaller and smaller as B differed more and more from A! This suggests again that these are not repetitions at all, but rather *near returns* of the solutions to their initial conditions, which occur after a number of turns $N(l)$ that increases linearly with l, just as in the case of the *exact returns* of the integrable system shown in figure 5. On the other hand, turning around one pair of singularities, we always found exact returns, as in the Calogero–Moser case.

This evidence shows that, in non-integrable Hamiltonian systems with only algebraic singularities, the ISS predicted by Ziglin's theorem [6, 12] can be found, when integrating around suitably large contours in the complex t-plane. The branches of the multitude of singularities encountered on different sheets apparently become connected in such a way that the solutions are no longer allowed to repeat after the number of turns expected from the integrable case.

Of course, whether what we have just described is evidence of true ISS cannot be decided by numerical computations alone. Although we have observed that the (absolute) differences of the solutions from their initial values keep growing steadily by nearly the same amounts for several hundreds of turns, we cannot be sure that this trend will continue and these differences will not become zero (after a few more hundreds of turns), leading eventually to finitely sheeted solutions.

Concluding this section, we wish to add that entirely similar results as described above are found in two other potentials of this class:

(i) potential (1.2) with (1.3*c*), which is *smooth* for all real (x, y);

(ii) potential (1.2), with (1.3*b*), *but with* $k < 0$, which describes *unbounded* motion in the region $x^2+y^2<1$.

In system (ii), solutions are different than in the $k>0$ case and the equations of motion (4.3) had to be numerically integrated anew to observe iss for $A = B$ and obtain figures very similar to figure 5, found for $k>0$.

On the other hand, for system (i), no new integration is needed since it can be directly derived from the potential (1.2) with (1.3*b*), $k>0$, by the canonical transformation of variables:

$$x=\mathrm{i}x' \qquad y=\mathrm{i}y' \qquad p_x=-\mathrm{i}p'_x \qquad p_y=-\mathrm{i}p'_y \qquad t=-t' \qquad H=-H' \tag{4.7}$$

where H, H' are the Hamiltonians of the two systems. Clearly, with (4.7) the solutions of one system are mapped to those of the other, at the same parameter values A, B, in such a way that their corresponding analytical properties in complex t are identical.

5. The Grammaticos–Dorizzi–Ramani potential

We now turn to a Hamiltonian system of two degrees of freedom:

$$H(x, y, p_x, p_y)=\tfrac{1}{2}(p_x^2+p_y^2)+V(x, y) \tag{5.1}$$

with

$$V(x, y)=\tfrac{1}{8}x^4+\tfrac{3}{4}x^2y^2+y^4+\lambda x \tag{5.2}$$

whose singularity analysis was first carried out by Grammaticos *et al* [6, 11]. This potential, for $\lambda=0$, near a singularity $t=t_*$ has solutions of the following type:

$$\text{(i)} \qquad x=2\sqrt{5}\,\tau^{-1}+\sum_{n=0}^{\infty}a_n\tau^n \qquad y=2\mathrm{i}\sqrt{2}\,\tau^{-1}+\sum_{n=0}^{\infty}b_n\tau^n \tag{5.3}$$

$$\text{(ii)} \qquad x=2\mathrm{i}\,\tau^{-1}+\sum_{n=0}^{\infty}c_n\tau^n \qquad y=d\tau^3+\sum_{n=4}^{\infty}d_n\tau^n \tag{5.4}$$

$$\left.\begin{aligned}\text{(iiia)} \qquad & x=f\tau^{-1/2}+\tau^{1/2}\sum_{n=0}^{\infty}f_n\tau^n\\ \text{(iiib)} \qquad & x=h\tau^{3/2}+\tau^{3/2}\sum_{n=1}^{\infty}h_n\tau^n\end{aligned}\right\} \qquad y=\frac{\mathrm{i}}{\sqrt{2}}\tau^{-1}+\sum_{n=0}^{\infty}g_n\tau^n \tag{5.5}$$

$\tau=t-t_*$ where d, f and h are arbitrary constants. It possesses the Painlevé property in the variables $X=x^2$, $Y=y$, since the apparent square root singularities in (5.5) are trivially removed by squaring x. The second integral, in the $\lambda=0$ case, is [11]

$$C=p_x^4+(24x^2y^2+4x^4)p_x^2-16x^3yp_xp_y+4x^4p_y^2+4x^8+16x^6y^2+16x^4y^4. \tag{5.6}$$

Remarkably enough, when $\lambda\neq 0$ in (5.2), the *only* qualitative change in (5.3)–(5.5) is the appearance, in the expansions for x in (5.5), of *all* the powers of $\tau^{1/2}$ (hence integer powers of τ also). This precludes the simple removal of half-integer powers by squaring, eliminates the integral (5.6) and renders the problem non-integrable, as shown by the presence of large-scale chaotic regions on its surfaces of section [15].

Furthermore, no logarithmic terms arise in that case, as all compatibility conditions associated with the free constants in the series (5.3)–(5.5) are satisfied for all λ. Thus (5.2), with $\lambda \neq 0$, is another example of a non-integrable potential, whose 'worst' singularities are (locally) of the square root type. Its only distinctive feature is the fact that, unlike the potentials of sections 3 and 4, these singularities are *infinite* (i.e. x, y diverges at finite $t = t_*$), as they are produced by a potential (5.2), which is an entire function of x and y.

We have also integrated the equations of motion of this system numerically in the complex t-plane and have found here the same results as in the previous sections: evaluating x, y, p_x, p_y around contours enclosing one complex conjugate pair of singularities (of the primary sheet) we find finitely sheeted solutions, while around two such pairs we found again evidence of ISS.

As before, the solutions exhibited near returns after a number of turns that increased linearly with the vertical side of the contours. Note in figure 6 the interesting pattern of singularities encountered on the different sheets. The appearance of clustering is, of course, illusory since all these singularities are shown, in that figure, projected on the same sheet.

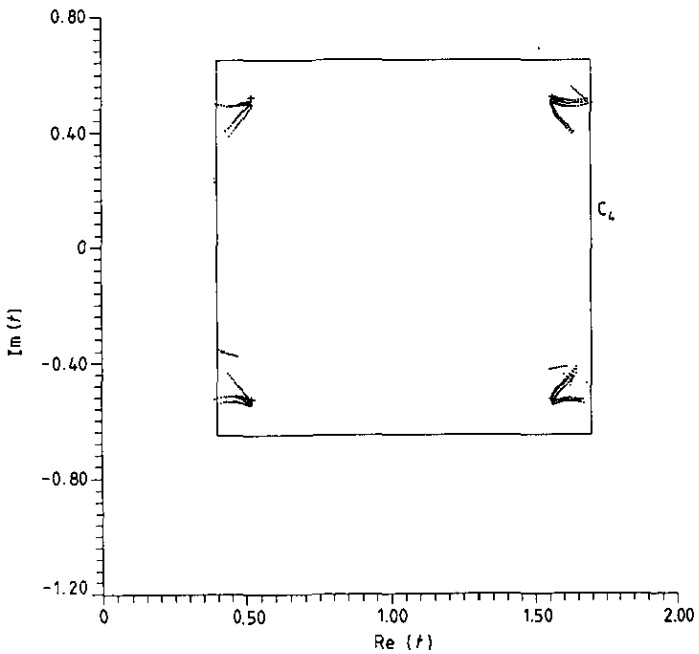

Figure 6. Singularity patterns for Hamiltonian (5.1) with (5.2) in the non-integrable case $\lambda = 0.02$, observed when integrating around a contour C_4 enclosing two singularity pairs.

6. The weak-Painlevé potentials (1, 5)

We finally turn to the analysis of the sheet structure of the solutions of an interesting class of completely integrable systems with only algebraic singularities: the weak-Painlevé potentials [6, 16], whose finite branching cannot be removed by simple coordinate transformations [17].

In particular, we will concentrate here on two examples of a family of such potentials

$$V_n(x, y) = \sum_{k=0}^{[n/2]} 2^{-2k} \frac{(n-k)!}{k!(n-2k)!} x^{2k} y^{n-2k} \tag{6.1}$$

(where $[\ldots]$ denotes the integer part) namely the $n = 5$ and $n = 6$ cases,

$$V_5 = y^5 + y^3 x^2 + \tfrac{3}{16} y x^4 \tag{6.2}$$

$$V_6 = y^6 + \tfrac{5}{4} x^2 y^4 + \tfrac{3}{8} x^4 y^2 + \tfrac{1}{64} x^6 \tag{6.3}$$

examine the analytic structure of their solutions and compare the results with what we have found in previous sections.

Starting, for example, with (6.2), one notes from its equations of motion (with $V_5 \to -V_5$)

$$\ddot{x} = 2xy^3 + \tfrac{3}{4} y x^3 \qquad \ddot{y} = 5y^4 + 3x^2 y^2 + \tfrac{3}{16} x^4 \tag{6.4}$$

that, at leading order, the behaviour of the solution near a singularity at $t = t_*$ belongs to one of the following types:

(i) $x, y \approx (t - t_*)^{-2/3}$ as $t \to t_*$ (6.5*a*)

(ii) $y \approx (t - t_*)^{-2/3}$ $x \approx (t - t_*)^p$ with $p = -\frac{1}{3}$ or $\frac{4}{3}$. (6.5*b*)

Moreover, this system has the second integral of motion [6, 18]

$$I = -y p_x^2 + x p_x p_y - \tfrac{1}{2} x^2 y^4 + \tfrac{3}{8} x^4 y^2 - \tfrac{1}{32} x^6. \tag{6.6}$$

Note that the rational powers in the expansions of x, y to higher orders in (6.5) cannot be trivially transformed away by taking the cubic powers of x, y, as these expansions contain, in general, all powers of $(t - t_*)^{1/3}$.

In fact, all potentials (6.1) have a second integral quadratic in the velocities, are separable in parabolic coordinates but do not belong to the class of potentials found by Whittaker [16]. It is known, however, that it is quite difficult to obtain explicit solutions of (6.4) as functions of t.

Now potential (6.2) has no local minimum about which the particle can execute bounded oscillations, hence no periodic array of singularities is found on the primary sheet in this case. There is, however, one pair of singularities on the primary sheet.

Integrating the equations of motion (6.4) numerically in the complex t-plane around this pair of singularities, along contours with vertical side l, we found that the solutions exactly returned to their starting values, after a number of turns N which increases linearly with l.

Finally, we studied the weak-Painlevé potential V_6, which does support real, bounded oscillations about its minimum at $x = y = 0$. Integrating its equations of motion

$$\begin{aligned} \ddot{x} &= -\tfrac{5}{2} x y^4 - \tfrac{3}{2} x^3 y^2 - \tfrac{3}{32} x^5 \\ \ddot{y} &= -6y^5 - 5x^2 y^3 - \tfrac{3}{4} x^4 y \end{aligned} \tag{6.7}$$

around singularities, at which the solutions diverge like $(t - t_*)^{-1/2}$ and $(t - t_*)^{-1/4}$, we always found finitely sheeted solutions and linear growth of the number of turns $N(l)$ (at which the solutions repeat) as a function of the 'height' of the contours l, around one complex conjugate pair of singularities (see figure 7(*a*)).

Interestingly enough, however, around two such singularity pairs $N(l)$ becomes a piecewise constant function of l, as seen in figure 7(*b*). Whether these results are generally valid for the whole class of weak-Painlevé potentials (6.1) is currently a matter under investigation.

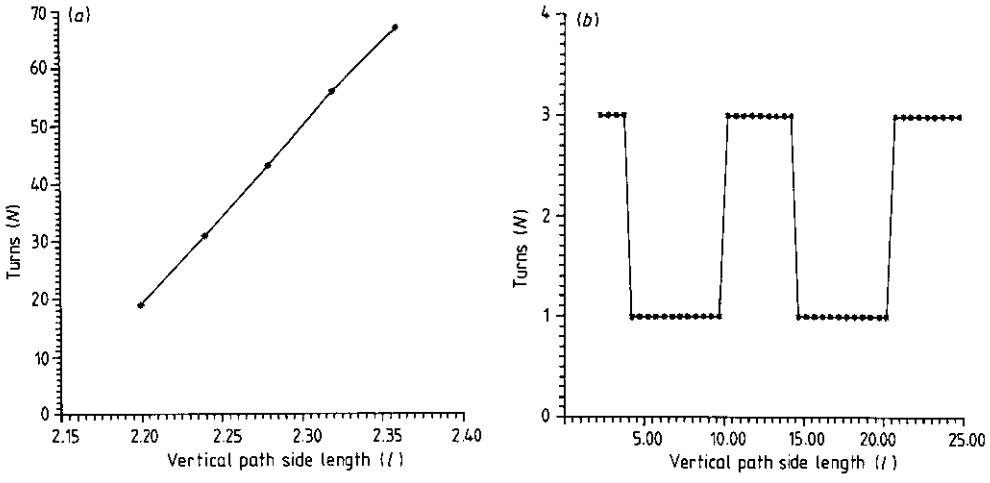

Figure 7. Plot of the number of turns N needed to (exactly) return to the original Riemann sheet versus the length of the vertical side of contours (a) around one pair and (b) around two pairs of singularities for the weak-Painlevé potential (6.3).

8. Discussion and conclusion

In recent years, the connection between (non-)integrability of dynamical systems and the analytic structure of their solutions in the complex t-plane has been the subject of intense investigation. As expected, the literature on *integrable* systems (whose solutions have *only poles* in complex t) grew disproportionately at first, yielding many new integrable examples as well as a number of rigorous results, on N-degree of freedom Hamiltonian systems, using the powerful techniques of algebraic geometry [19].

On the other hand, at the forefront of research on non-integrable systems, progress has been slower. The presence of ISS in such systems was noted early enough, when it was observed that *logarithmic* singularities typically occurred in perturbations of integrable systems [20]. However, the *necessity* of ISS for non-integrability was rigorously established somewhat later, with the work of Ziglin [6, 12] and Yoshida [6, 21] on Hamiltonian systems with *infinitely branched* singularities. Furthermore, such singularities have been seen to *cluster* on the same sheet in the complex t-plane [4–7], leading some to wonder whether this is also a necessary feature of non-integrability.

In this paper, we have presented arguments and numerical evidence demonstrating that infinite branching and clustering of singularities are *not necessary* for non-integrability. On the other hand, we found that ISS *are* necessary, as infinitely many sheets always appear to exist, in non-integrable systems with only algebraic singularities, when the equations of motion are integrated along suitably large contours in the complex t-plane.

A very important class of dynamical systems with only algebraic (typically square root) singularities in complex time are those whose singularities are *finite*, i.e. occur at finite values of their configuration coordinates x, y, cf (1.1) with (1.2). Near such values, the potential of the problem $V(x, y) \sim k(f(x, y))^{-2}$ rises sharply to infinity and, in the limit of $k \to 0$, strongly resembles a model of hard *billiards* [22].

One of the objectives of this research is to use singularity analysis, at the $k \to 0$ limit, to study the solutions of the physically interesting *real* billiards, using *complex billiards*, where collisions are viewed as square root singularities around which the solutions can be analytically continued in complex time [23]. Analysing the sheet structure of a hard billiard case, it may thus be possible to understand the behaviour of solutions of a large class of *soft* billiards (be they integrable or not) which have the same hard billiard limit.

Finally, the results presented in this paper lead us to conjecture that dynamical systems possessing only algebraic singularities are integrable if and only if their solutions, around any finite-size contour in the complex t-plane, are always finitely sheeted. Evidence of ISS is often numerically obtained around short enough contours (in all our cases enclosing two complex conjugate pairs was sufficient), to provide a practical criterion for non-integrability, especially for systems whose real time motion appears very regular on surfaces of section (as is the case with the soft billiards of section 4 for $x^2+y^2<1$).

Of course this criterion becomes more useful near integrable cases where the trend towards ISS can be more easily detected along relatively short integration paths in the complex t-plane. A more important point, however, remains the need for rigorous justification of the above results, which is currently under investigation on perturbations of some special integrable cases, where the analytic structure is explicitly known (see appendix 2).

Acknowledgments

We wish to thank R Mondragon, R Broucke, A Arneodo, L Reichl and P Morisson for many useful discussions and acknowledge the financial support of the EEC Science/Stimulation Program, under contrast SCI-0156, and the UK Science and Engineering Research Council. Part of this work was carried out while one of us (TB) was a visiting professor at the Center of Statistical Mechanics and Complex Systems, and Institute for Fusion Studies, of the University of Texas at Austin, Texas, whose hospitality is gratefully acknowledged here.

Appendix 1. Numerical methods and results

In this appendix, we provide further details concerning the numerical results presented in this paper. These results were obtained by integrating the equations of motion of each problem along piecewise linear (closed or open) contours in the complex t-plane, using the ATOMFT package. This package, originally developed by Chang and Corliss [13] as ATOMCC, was further improved and successfully employed in recent years to exhibit in a most graphic way the fascinatingly complicated singularity patterns of non-integrable systems [4–8].

As is well known, this numerical package is designed to solve a system of ordinary differential equations in the complex plane of their independent variable t, by expanding the solutions in Taylor series and determining, at every step, its circle of convergence in the t-plane. The intersection points of all these circles provide, of course, the locations of singularities $t = t_*$, like the ones shown in figures 1, 4 and 6.

The variable step size $t \to t + h$ of the integration procedure is internally determined depending on the distance of t from the nearest t_*. The number of terms in the Taylor

series may also be varied (we have taken up to 140, in some cases) in order to specify, as accurately as possible, the *location* of the *nearest* t_* and the *power* α, in the leading order $(t-t_*)^\alpha$ $(\alpha<0)$, by which the position (or momentum) variables diverge at $t=t_*$. These two numbers are generally obtained within 4–5 digit accuracy.

An important point to remember is that the ATOMFT package provides, at every step, the location of the singularity *nearest* to its integration path, at that value of t. Thus, care must be taken in turning around a certain t_* to distinguish between singularities lying on different sheets! In figures 4 and 6, for example, we marked by crosses (×) the singularities on the first (primary) sheet and by dots (·) all those appearing on the higher sheets.

Our numerical integrations around contours of the type C_1, C_4 (see figure 1) proceeded in the following way. Starting with initial conditions at the origin of the complex t-plane we integrated to the point P on the upper left-hand corner of our contours and recorded the value of the solutions there:

$$X_0(P)=(x_0(P),\, y_0(P),\, p_{x_0}(P),\, p_{y_0}(P)). \tag{A1.1}$$

We then started integrating around the contour (always in the clockwise direction) and recorded at P, after the ith turn, the values

$$X_i(P)=(x_i(P),\, y_i(P),\, p_{x_i}(P),\, p_{y_i}(P)) \qquad i=1,2,\ldots. \tag{A1.2}$$

To check whether we had returned to the original sheet we computed, after every turn,

$$\Delta X_i(P)=X_i(P)-X_0(P) \qquad i=1,2,\ldots \tag{A1.3}$$

and, in particular, the absolute differences of the x variable:

$$|\Delta x_i(P)|=|x_i(P)-x_0(P)| \qquad i=1,2,\ldots. \tag{A1.4}$$

In all the integrable cases studied in this paper, these differences became zero (within the accuracy of our computations) i.e. 10^{-14}–10^{-10}, with the errors growing *as* the *size* of the contour (i.e. the height of the rectangles $PP'=l$ in figure 1) increased further and further. For all integrable potentials (except the Calogero–Moser one) (A1.4) becomes zero, after a number of turns N that increases linearly with l (see sections 4–6 for more details).

On the other hand, when $A\neq B$ and our potentials become non-integrable, evidence of ISS is observed in the following way. Computing the differences (see (A1.4)) for $i=N, 2N, 3N,\ldots$ we noted that they were no longer zero, but began to increase, after every N turns, by *nearly the same amount*, i.e.

$$|\Delta x_{kN}(P)|\approx k\delta_x \qquad k=1,2,\ldots. \tag{A1.5}$$

The values of δ_x (and those of δ_y, δp_x, δp_y of the corresponding differences of the variables y, p_x, p_y), of course, tend to zero in the integrable limit $A\to B$.

It is important to note, however, that this evidence of ISS was obtained around contours C_4 containing two complex conjugate pairs of singularities. When we integrated around one pair we always found $|\Delta x_{kN}(P)|=0$, within the accuracy of our calculations. Furthermore, we verified all of these results by integrating around many contours hundreds of times, checking our numerical errors, e.g. by the variation of the energy integral.

The presence of ISS becomes more and more evident as B is changed further and further away from the case $B=A$. In table 1, we list some typical results for the Calogero–Moser and soft billiard potentials, showing how solution differences grow,

Table 1. Typical results for Calogero-Moser and soft billiard potentials ($A=1$, $l=0.6$).

	B					
$\lvert\Delta x_N\rvert$ for	1.000 01	1.0001	1.001	1.01	1.15	1.5
Soft billiards		1.035×10^{-5}	0.956×10^{-4}	0.883×10^{-3}	0.7689×10^{-2}	0.7098×10^{-1}
Calogero-Moser	0.1635×10^{-5}	0.1635×10^{-4}	0.1637×10^{-3}	0.1656×10^{-2}	0.297×10^{-1}	

as B grows, and how this trend to (or away from) finite-sheetedness can be used to single out parameter values at which a dynamical system with only algebraic singularities is integrable.

Appendix 2. An exactly solvable soft billiard problem

As we noted in section 4 the soft billiard Hamiltonian

$$H=\tfrac{1}{2}(\dot{x}^2+\dot{y}^2)+\tfrac{1}{2}(Ax^2+By^2)+\frac{k}{(x^2+y^2-1)^2} \qquad k, A, B>0 \tag{A2.1}$$

is integrable for $A=B$, since it is separable in polar coordinates $x=r\cos\theta$, $y=r\sin\theta$, in terms of which the energy equation is

$$\frac{1}{2}\left(\frac{\mathrm{d}r}{\mathrm{d}t}\right)^2+\frac{A}{2}r^2+\frac{J^2}{2r^2}+\frac{k}{(r^2-1)^2}=E \tag{A2.2}$$

where $J=r^2\dot{\theta}=\text{const.}$ is the angular momentum integral. Separating r and t in (A2.2) and introducing the new variable

$$u=r^2-1 \tag{A2.3}$$

we obtain after some manipulation

$$t-t_0=\pm\tfrac{1}{2}\int_{u_0}^{u}\frac{u\,\mathrm{d}u}{\sqrt{2E(u+1)u^2-A(u+1)^2u^2-J^2u^2-2k(u+1)}} \tag{A2.4}$$

which is our (4.4).

Collecting terms in the denominator we may write the integral of (A2.4) in the form

$$t-t_0=\pm\frac{\mathrm{i}}{2\sqrt{A}}\int_{u_0}^{u}\frac{u\,\mathrm{d}u}{\sqrt{u^4+\alpha u^3+\beta u^2+\gamma u+\delta}} \tag{A2.5}$$

with

$$\alpha=2-\frac{2E}{A} \qquad \beta=1-\frac{2E}{A}+\frac{J^2}{A} \qquad \gamma=\frac{2k}{A} \qquad \delta=\frac{2k}{A}. \tag{A2.6}$$

The integral in (A2.5) can now be expressed in terms of elliptic integrals of the first and third kind,

$$F(\varphi,\lambda)=\int_0^{\sin\phi}\frac{\mathrm{d}x}{\sqrt{(1-x^2)(1-\lambda^2x^2)}} \tag{A2.7a}$$

$$\Pi(\varphi,\nu,\lambda)=\int_0^{\sin\phi}\frac{\mathrm{d}x}{(1-\nu x^2)\sqrt{(1-x^2)(1-\lambda^2x^2)}} \tag{A2.7b}$$

depending on the location of its upper and lower limit, with respect to the roots of the polynomial in the denominator (see [14], section 3.148). For example,

$$\int_a^v \frac{u\,du}{\sqrt{(u-a)(u-b)(u-c)(u-d)}}$$

$$= \frac{2}{\sqrt{(a-c)(b-d)}}\left[(a-b)\Pi\left(\varphi, \frac{a-d}{b-d}, \lambda\right) + bF(\varphi, \lambda)\right]$$

for $v > a > b > c > d$, with

$$\varphi = \sin^{-1}\sqrt{\frac{(b-d)(v-a)}{(a-d)(v-b)}} \qquad \lambda = \sqrt{\frac{(b-c)(a-d)}{(a-c)(b-d)}}$$

where u, v and all parameters a, b, c, d are real.

Since it appears quite difficult, in general, to invert the integral (A2.4), obtain explicitly $u = u(t)$ and study its sheet structure, we shall do that below in a special case in which the expression in the radical of (A2.4) and (A2.5) becomes a complete square, i.e. where

$$t - t_0 = \pm\frac{\mathrm{i}}{2\sqrt{A}}\int_{u_0}^{u}\frac{u\,du}{(u-\rho_1)(u-\rho_2)}. \tag{A2.8}$$

Evaluating this integral one finds

$$t - t_0 = \pm\frac{\mathrm{i}}{2\sqrt{A}}\frac{1}{(\rho_1-\rho_2)}\ln\left(\frac{(u-\rho_1)^{\rho_1}}{(u-\rho_2)^{\rho_2}}\right). \tag{A2.9}$$

To achieve this reduction we require that ρ_1, ρ_2 satisfy

$$\pm\sqrt{2kA}\,\rho_2^2 + k\rho_2 + 2k = 0 \tag{A2.10a}$$

$$\rho_1 = \pm\sqrt{\frac{2k}{A}}\frac{1}{\rho_2}. \tag{A2.10b}$$

$$E = A(1+\rho_1+\rho_2) \tag{A2.10c}$$

$$J = \pm\sqrt{2E - A(1-\rho_1^2-\rho_2^2-4\rho_1\rho_2)}. \tag{A2.10d}$$

To further simplify the algebra we choose $A = 2/k$, whence (A2.10a, b) become

$$\pm 2\rho_2^2 + k\rho_2 + 2k = 0 \tag{A2.11a}$$

$$\rho_1 = \pm\frac{k}{\rho_2}. \tag{A2.11b}$$

We now have two choices:

(i) $\rho_1\rho_2 < 0$, with the minus sign in (A2.11), and thus we have

$$\rho_1 = \frac{k+\sqrt{k^2+16k}}{4} \qquad \rho_2 = \frac{k-\sqrt{k^2+16k}}{4}$$

$$E = 1+\frac{2}{k} \qquad J^2 = -2+\frac{2}{k}+\frac{k}{2} \tag{A2.12}$$

(ii) $\rho_1\rho_2>0$, with the plus sign in (A2.11*a*, *b*), and thus we have

$$\rho_1=\frac{-k+\sqrt{k^2-16k}}{4} \qquad \rho_2=\frac{-k-\sqrt{k^2-16k}}{4}$$
$$E=-1+\frac{2}{k} \qquad J^2=2+\frac{2}{k}+\frac{k}{2}. \tag{A2.13}$$

Taking now $k=1$, (A2.12) gives, in case (i),

$$\rho_1=\frac{1+\sqrt{17}}{4} \qquad \rho_2=\frac{1-\sqrt{17}}{4} \qquad E=3 \qquad J=\frac{1}{\sqrt{2}} \tag{A2.14}$$

and, in case (ii),

$$\rho_1=\frac{-1+\mathrm{i}\sqrt{15}}{4} \qquad \rho_2=\frac{-1-\mathrm{i}\sqrt{15}}{4} \qquad E=1 \qquad J=\frac{3}{\sqrt{2}}. \tag{A2.15}$$

Inserting ρ_1, ρ_2 from (A2.14) in (A2.9), for $t_0=0$, and splitting real from imaginary parts we find for the imaginary part of a singularity $t_*=t_R+\mathrm{i}t_I$ (at which $r^2=1$):

$$t_I=\pm\frac{1}{4\sqrt{34}}\left[(1+\sqrt{17})\ln\left(\frac{1+\sqrt{17}}{4}\right)-(1-\sqrt{17})\ln\left(\frac{1-\sqrt{17}}{4}\right)\right]. \tag{A2.16}$$

Integrating now numerically along some path, with initial conditions satisfying (A2.14), we found, in complete agreement with (A2.16), that no new singularities appear as one keeps turning around contours enclosing singularities of the primary sheet.

On the other hand, in case (ii), with (A2.15), we similarly find a *multitude* of singularities t_*, lying on *different* sheets, whose imaginary parts satisfy

$$t_I=\pm\frac{1}{2\sqrt{30}}(\cos^{-1}\tfrac{1}{4}+m\pi) \qquad m=0,\pm1,\pm2,\ldots \tag{A2.17}$$

in agreement with what finds integrating numerically equations of motion in the complex t-plane.

References

[1] Yoshida H 1983 *Celest. Mech.* **31** 363, 381
[2] Yoshida H, Ramani A and Grammaticos B 1987 *Acta Appl. Math.* **8** 75
[3] Dombre T *et al* 1986 *J. Fluid Mech.* **167** 353
[4] Bountis T, Papageorgiou V and Bier M 1987 *Physica* **24D** 292
[5] Fournier J D, Levine G and Tabor M 1988 *J. Phys. A: Math. Gen.* **21** 33
[6] Ramani A, Grammaticos B and Bountis T 1989 *Phys. Rep.* **180**(3) 160
[7] Chang Y F, Tabor M and Weiss J 1983 *J. Math. Phys.* **23** 531; 1982 *Physica* **8D** 380
[8] Tabor M and Weiss J 1981 *Phys. Rev.* A **24** 2157
[9] Olshanetsky M A and Perelomov A M 1981 *Phys. Rep.* **71** 313
[10] Bountis T, Drossos L and Percival I C 1990 Non-integrable systems with square root singularities in complex time *Preprint*
[11] Grammaticos B, Dorizzi B and Ramani A 1983 *J. Math. Phys.* **24** 2289
[12] Ziglin S L 1982 *Trans. Moscow Math. Soc.* **1** 283
[13] Chang Y F and Corliss G 1980 *J. Inst. Math. Appl.* **25** 349
[14] Gradshteyn I S and Ryzhik I M 1980 *Tables of Integrals, Series, and Products* (London: Academic)
[15] Dorizzi B 1983 *Thèse d'Etat* Orsay

[16] Dorizzi B, Grammaticos B and Ramani A R 1983 *J. Math. Phys.* **24**(9) 2282
[17] Hietarinta J *et al* 1984 *Phys. Rev. Lett.* **53**(18) 1707
[18] Ramani A, Dorizzi B and Grammaticos B 1982 *Phys. Rev. Lett.* **49** 1538
[19] Adler M and van Moerbeke P 1988 *Algebraically Completely Integrable Systems: a Systematic Approach, Perspectives in Mathematics* (Boston: Academic)
[20] Bountis T and Segur H 1988 *AIP Conf. Proc.* vol 88 (New York: AIP) p 279
[21] Yoshida H 1987 *Physica* **29D** 128; 1989 *Phys. Lett.* **141A**(3, 4) 108
[22] Vivaldi F and Shaidenko A 1987 *Commun. Math. Phys.* **110** 625
[23] Mondragon R and Percival I 1990 Complex billiards and soft billiards *Preprint*